Digest Journal of Nanomaterials and Biostructures Vol. 11, No. 1, January - March 2016, p. 149 - 157

EFFECT OF MULTIWALLED CARBON NANOTUBES ON Co-Mn FERRITE PREPARED BY CO-PRECIPITATION TECHNIQUE

A. HAKEEM[a], G. MURTAZA[b,,c*], I. AHMAD[b], P. MAO[c], X. GUOHUA[c], M. T. FARID[b], M. KANWAL[b], G. MUSTAFA[b], M. HUSSAIN[c], M. AHMAD[d]
[a]*Department of Physics, Govt. Post Graduate College Jampur, Pakistan*
[b]*Department of Physics, Bahauddin Zakariya University, Multan 60800 Pakistan*
[c]*Department of Polymer Science and Engineering, Zhejiang University, Hangzhou 310037 PR China*
[d]*Department of Physics, COMSATS Institute of Information Technology, Lahore 54000, Pakistan*

Multiwalled carbon nanotubes (MWCNTs) are substituted in the soft ferrite $Co_{0.5}Mn_{0.5}Fe_2O_4$, with weight percent ratio of 1%, 5% and 9%. The effect of MWCNTs on the Structural, Thermal and Magnetic properties of Co-Mn ferrites is reported. The X-ray diffraction analysis reveals the ferrite posses spinel cubic structure. Structural, Thermal analysis of the MWCNTs and Co-Mn ferrite composite are characterized by XRD, SEM and TGA/DSC techniques. The sintered powder at 1000°C under atmospheric environment shows spinel cubic structure. Particle size is observed by SEM ranging from 20 nm to 35nm. The magnetic properties are measured by using the Physical property measurements (PPMS) technique. The Fourier transform infrared spectroscopy detects the presence of the metallic compounds in the ferrite sample.

(Received December 9, 2015; Accepted February 8, 2016)

Keywords: X-ray scattering; differential scanning calorimetry (DSC); Fourier transform infrared spectroscopy (FTIR); Thermo gravimetric analysis (TGA).

1. Introduction

The third allotrope was carbon nanotubes (CNTs), next to diamond and graphite which were discovered in 1991[1].These possesses remarkable properties such as extremely high tensile strengths (150-180GPa), ballistic thermal conduction (>300 w/mK for individual tubes), electric modulus (640Gpa to 1Tpa) and high electrical conductivity [2-5] have been unveiled. To make high frequency transformers, chokes, inductor coils, cores of audio frequency, magneto optical displays, microwave absorbers, permanent magnets, gas sensors and wave guides in GHz range were mostly prepared by ferrites [6, 7]. The synthesis process of MWCNTs/Ferrites started later as compared to MWCNTs/Polymer composites but it is not developed yet. The MWCNTs/Ferrite composites were prepared by a solid state reaction method. The well known magnetic compounds are ferrites that have been studied for the potential application in magnetic recording media and in microwave absorber devices due to their novel physical properties [8-11]. In the recent years studies on the properties of Nano sized ferrite particles have drawn considerable interest because of their fundamental importance in understanding the physical processes and their applications for many technological purposes. Cobalt ferrites have emerged as one of the important ferromagnetic materials because of their low eddy current losses and high electrical resistivity. These have cubic spinel structure and are being extensively studied on the basis of their interesting magnetic and electrical properties. The structural stability of the Nano sized particles of cobalt ferrite plays an important role in technical applications. The chemical method of preparation has a great impact on the physical and structural properties of the Nano sized constituents. The well chemical

*Corresponding author: mrkhichi@gmail.com

homogeneity in the Nano sized particles can be achieved by mixing them at the molecular level. The synthesis of Nano sized particle has a major impact on the shape and size distribution. The chemical routes of Nano sized particle preparation have emerged as a popular tool of synthesis for spinel ferrites. Nano sized particles can be obtained by using the various preparation methods. Among these the well known method of preparations of Nano sized particles are hydrothermal synthesis [12-15], co-precipitation [16-20], sol-gel [21-24], spray drying [25], solid state micro emulsion processes [26-28] and mechanical alloying [29-32]. Spinel ferrites have a numerous applications in different fields like Ferro fluids, magnetic recording, magnetic resonance imaging (MRI) and hot gas desulphurization etc. [33-36]. Spinel ferrites have the structural formula M $Fe_2O_4$where M is divalent metal ion from the 3d transition elements like Cu, Ni, Zn, Co, Mn etc, and a unit cell has 32 oxygen atoms in a cubic closest packing while octahedral and tetrahedral sites are available for cations [37, 38]. Normally in a spinel structure, divalent M^{2+}cation enter at the tetrahedral sites, and Fe^{3+}ions occupy the octahedral sites. Intermediate configurations are generally temperature dependent and are commonly defined by the inversion coefficient [38]. Co-precipitation method is chosen in the present work for preparing Co-Mn ferrites. As it is easy and convenient method to produce homogeneous Nano ferrites. It is well known fact that the ferrites intrinsic properties largely depend on the method of preparation, chemical composition and cation distribution. Crystalline structure of the composite Nano particles is characterized by XRD and scanning electron microscope (SEM). The FT-IR spectrum of the ferrite sample is recorded to make sure of the presence of the metallic compounds.

2. Experimental method and calculations

2.1 Materials

All the chemical re agents $Co(NO_3)_2.6H_2O$, $Mn(NO_3)_2.6H_2O$ and Ferric nitrate Nona hydrate $Fe(No_3)_3.9H_2O$ of Sigma Aldrich, Multiwalled carbon nanotubes (MWCNTs) were purchased from Shenzhen Nanotech Port Co. Ltd., and hydrochloric acid HCl, Nitric acid HNO_3 were of Merck co. Germany. These acids are used to purify the MWCNTs. The length and diameter of the MWCNTs were 20μm and 20nm, respectively.

2.2 Synthesis method

Nano crystalline Cobalt ferrites $Co_{0.5}Mn_{0.5}Fe_2O_4$ were prepared by co-precipitation method. The desired composition was obtained by taking stoichiometric amount of $Co(NO_3)_2.6H_2O$, $Mn(NO_3)_2.6H_2O$ and $Fe(NO_3)_3.9H_2O$ were dissolved in deionized water. Ammonia solution was used to make the precipitate. The pH value of the solution becomes 10 and it was stirred for at least 2hrs so that the solution becomes neutral. Put the solution in a sonicater for 20 minutes then place it in the ultrasonic bath for a while so that precipitate will settle down then filter it with a filter paper. Wash the precipitate with deionized water until it becomes free of impurities. The product was dried at 100ºC for 5 hours to remove water contents. The dried powder was calcinated at 1000ºC and mixed the ferrite with multiwall carbon nanotubes having weight percentage ratio of 1%, 5% and 9%. Several strategies have already been developed over the last decade to obtain MWCNTs as a pure as possible, and to minimize the influence of impurities on the performance of composites. Impurities can indeed affect the batch to batch reproducibility of the results, and accordingly influence on the properties of the final composite. The method we have used to purify the MWCNTs is by using the hydrochloric acid (HCl) and nitric acid (HNO_3) with 1:3 by volume as it is reported in the literature [39-41].

2.3 Characterization

The X-ray diffraction (XRD) patterns of the samples were recorded on a BRUKER X-ray powder diffractometer using CuKα (1.54060Å) radiation. The scans of the selected diffraction peaks were carried out in the step mode. Scherrer's method can be used to calculate the crystallite size of the particles [42]. Thermo gravimetric studies (TG) and differential scanning calorimetric studies (DSC) were done on SDTQ600 V8.2 Build 100, Module DSC-TGA standard, Inst Serial 0600-0109 and the heating rate was kept at 10 °C/min. The infra red (IR) spectrum of ferrite

sample was recorded on Shimadzu Model 8201, Fourier Transform infra red (FTIR) in the range of 4000cm^{-1} to 450cm^{-1} were recorded in the presence of KBr medium at room temperature. Magnetic properties were measured by PPMS ACMS Option Version 1.0.9 Build 14.

2.4 Calculations

The lattice constant 'a' was determined by using the following relation:

$$a = d_{hkl}\sqrt{h^2 + k^2 + l^2} \quad (1)$$

where d_{hkl} is the distance between the adjacent Millar planes (h k l). d_{hkl} can be calculated by the relation:

$$d_{hkl} = \frac{n\lambda}{2\sin\theta} \quad (2)$$

with n = 1 for the cubic system,
The X-ray density ρ_x can be calculated by the help of Smit and Wijin relation [43].

$$\rho_x = \frac{ZM}{Na^3} \quad (3)$$

Where M is the molecular weight and N is the Avogadro's number (6.023 x10^{23}atoms/mol), Z is the number of molecules pet unit cell (for oxide compounds with cubic spinel structure Z = 8) and 'a' is the lattice parameter in (cm). The average particle size was calculated by using the Scherrer's equation

$$D = \frac{0.9\,\lambda}{\beta\cos\theta} \quad (4)$$

Where D is crystallite size, λ is the wavelength of the X-ray radiation, θ is the Bragg's angle, and β is the line width at maximum height [44]. The porosity can be calculated by the following relation

$$P = \frac{\rho_x - \rho_m}{\rho_x} \quad (5)$$

Where ρ_x the density is calculated by Eq. (3), and ρ_m is the measured density. It can be calculated by the following relation.

$$\rho_m = \frac{M}{V} = \frac{M}{\pi r^2 t} \quad (6)$$

Where M is the mass, t is the thickness and r is the radius of the pellet.

The X-ray diffraction of sintered Cobalt-Maganese ferrite sample sintered at 1000ºC is subject to calculate the average particle size using Debye –Scherrer formula. The crystalline structures of composite Nano particles are characterized by Scanning Electron Microscope (SEM).

3. Results and discussions

The X-ray diffraction patterns of $Co_{0.5}Mn_{0.5}Fe_2O_4$ powders fired at 1000°C. The x-ray diffraction measurement shows that all peaks of $Co_{0.5}Mn_{0.5}Fe_2O_4$ consist with those of a typical spinel structure of a cobalt ferrite prepared by co-precipitation method. Fig.1 illustrates the XRD patterns of the ferrite, carbon nanotubes composites having weight percent 1%, 5% and 9%. The XRD pattern of the ferrite indicates that the material is based on cubic spinel crystal structure of ferrite. The average crystallite size was in the range of 20-35nm. The strong diffraction peaks at 2θ = 18.2°, 30.22°, 35.53°, 43.30°, 53.58°, 57.35°, 62.72°, 73.2°, 78.6° corresponds to (220), (311), (222), (400), (422), (511), (440), (533), (444) typical planes of Co-Mn ferrite spinel structures with face centered cubic phase according to the standard card JCPDS file no. 520278 [45, 46].

In the XRD of Multi wall carbon nanotube, the broadened peak at 2θ = 26.3º indicates that the carbon nanotubes are present and no deformation takes place in their structure. In Fig. 1 all the XRD patterns of the (a) ferrite (b) Multiwall Carbon Nanotubes (MWCNTs) (c) composite which is formed by mixing the ferrite with 1% weight ratio of multiwall carbon nanotubes (d) composite which is formed by mixing the ferrite with 5% weight ratio of multiwall carbon nanotubes (e) composite which is formed by mixing the ferrite with 9% weight ratio of multiwall carbon nanotubes. The XRD pattern of MWCNTs (JCPGS 01-0640) purified by HCl and HNO_3 with volume ratio 1:3 is shown in Fig. 1(b). The interplanner spacing corresponding to (002) plane is found to be 3.35Å like pure graphite. XRD patterns shows an increase in the intensity of (002) plane peak, when we have mixed only 1% of MWCNTs the (002) plane peak is not prominent but on increasing the further amount of MWCNTs the (002) plane peaks become prominent especially (100) plane peak and the main peak of the spinel cubic structure reduces in intensity due to the percentage increase in of multiwalled carbon nanotubes and the reduction of the grain size. It means that increasing amount of multiwall carbon nanotubes has a great influence on the structural properties of the ferrite. The Scanning Electron Microscope (SEM) images are shown in Fig. 2. The SEM image of a pure ferrite is shown in Fig. 2(a) and the images of the composites are shown in Fig. 2(b-d) having percentage of multiwall composite 1%, 5% and 9%, respectively. SEM images clearly indicate the increasing percentage of multiwalled carbon nanotubes. The SEM image of a pure multiwall carbon nanotube is shown in Fig. 2(e). The images show that the multiwall carbon nanotubes having hollow cylindrical structure make agglomerates. All the obtained results are presented in Table 1.

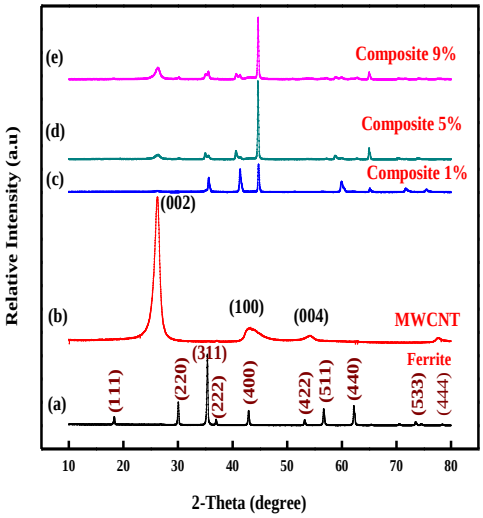

Fig. 1 XRD patterns of (a) Ferrite $Co_{0.5}Mn_{0.5}Fe_2O_4$, (b) Multiwall carbon nanotubes, (c) Composite with 1% MWCNTs, (d) Composite with 5% MWCNTs (e) Composite with 9% MWCNTs.

Table 1. The lattice parameter 'a', Crystallite Size D(nm), X-ray density(gm/cm^3), Actual density(gm/cm^3) and porosity values of Ferrite and composites are given below.

Sample Parameter	Ferrite	MWCNTs	Comp1%	Comp 5%	Comp 9%
Lattice Parameter 'a' (Å)	8.30		5.20	5.10	5.02
Crystallite Size D (nm)	35	20	30	28	25
X-ray density (gm/cm^3)	5.12		3.21	3.00	2.25
Actual density (gm/cm^3)	3.15	0.02	1.95	1.05	0.45
Porosity (%)	0.385		0.393	0.65	0.8

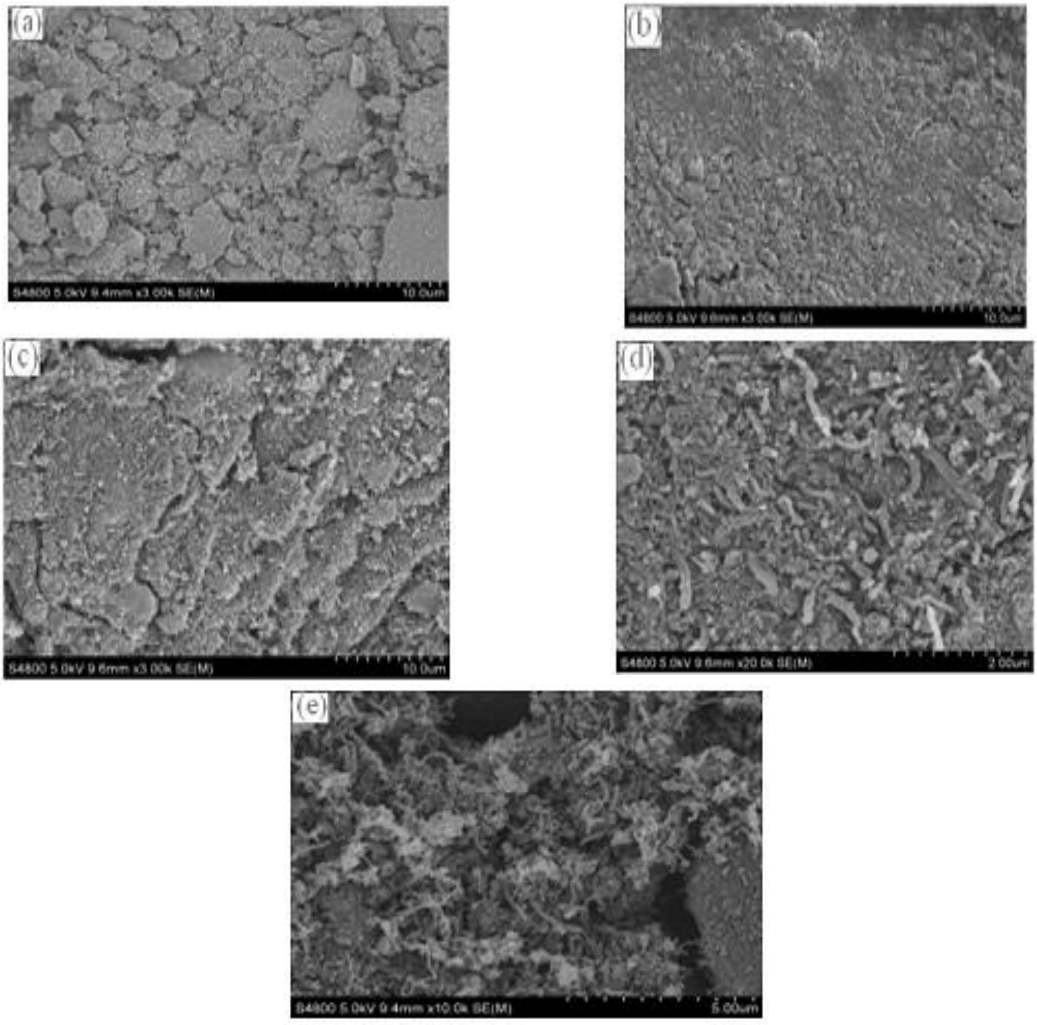

Fig.2 Scanning Electron Microscope (SEM) Images of (a) $Co_{0.5}Mn_{0.5}Fe_2O_4$,(b) $Co_{0.5}Mn_{0.5}Fe_2O_4$ MWCNTs 1% (c) $Co_{0.5}Mn_{0.5}Fe_2O_4$ MWCNTs 5%. (d) $Co_{0.5}Mn_{0.5}Fe_2O_4$ MWCNTs 9%, (e) MWCNTs.

Thermo gravimetric studies (TG) and differential scanning calorimetric studies (DSC) were done on SDTQ600 V8.2 Build 100, Module DSC-TGA standard, Inst Serial 0600-0109 and the heating rate was kept at 10 °C/min. TGA-graphs of the samples show maximum weight loss in the range of 500°C to 600°C. This may be due to dehydration/removal of OH ions and some organic residues left in the sample. DSC curve of the sample show exothermic peak at 636°C 626°C, 627°C and 628°C, respectively. It may be due to the removal of the hydrocarbon residuals. TG-DSC curves of the samples show the formation of crystalline phase in the temperature range 600 and above. The pure multiwall carbon nanotubes loss their weight after attaining a temperature of 500°C, the weight loss is 98.16 % which means that the material remains stable until 500°C temperature after it abruptly loss in weight takes place as it is depicted in Fig. 3(a).

The composite based on 1% carbon nanotubes gains 6.2% weight. The sample gains weight after 300°C and this process continues till 575°C and it again losses its weight after 626.26°C and the loss in weight is 3.8% and it again gains weight due to the presence of metallic ions that is shown in Fig. 3(b).

The composite based on 5% multiwall carbon nanotubes gains weight after 375°C up till a temperature of 550ºC. The increase in weight is 5.3% then it start to decrease till 650°C, the loss in weight is 23.1 % and it attains a stable position which is depicted in Fig. 3(c).

The composite based on 9% multiwall carbon nanotubes gains weight after 250°C and it gains a weight of 2.50% till 580°C then it again losses its weight of 43.3% till 650°C and later on

the weight increases abruptly. It's mean that loss in weight takes place after the addition of MWCNTs as it is depicted in Fig. 3(d). Multiwalled carbon nanotubes gain weight by the addition of ferrite particles.

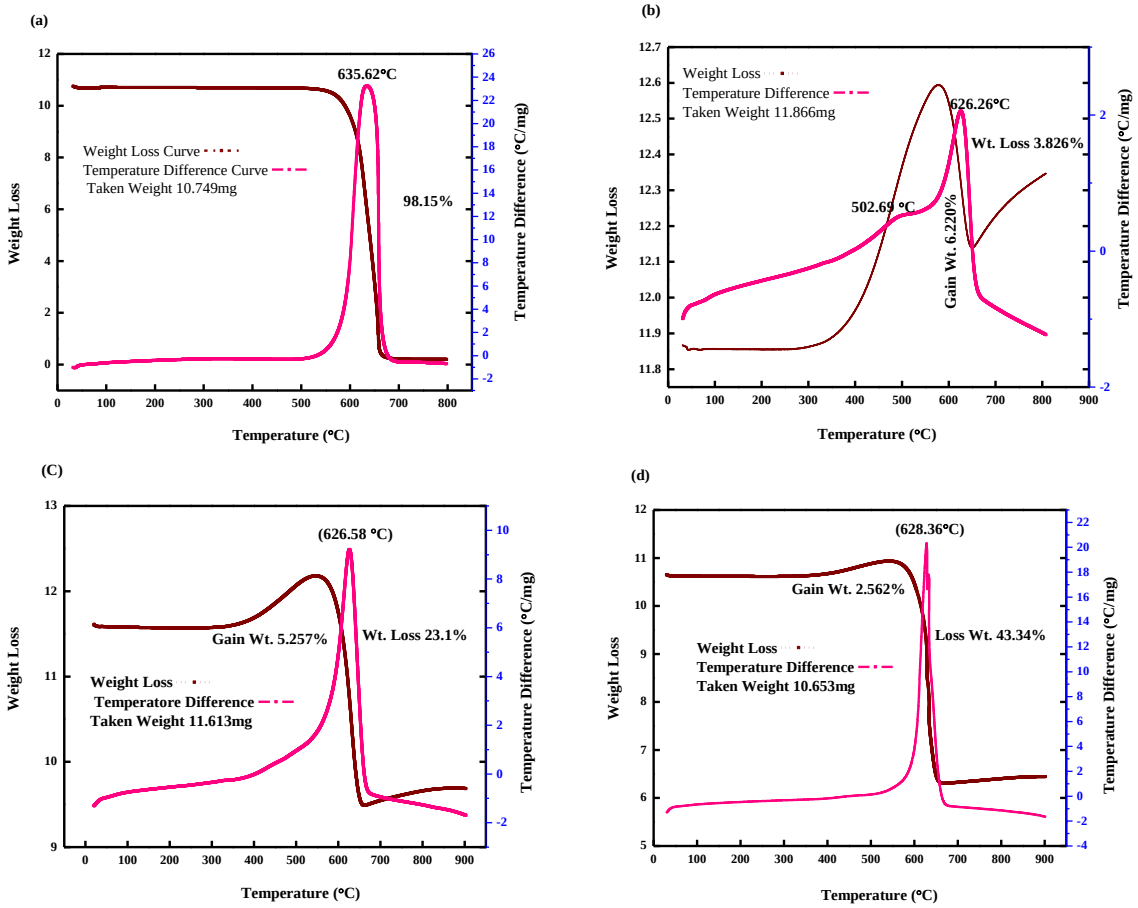

Fig. 3 Thermo gravimetric (TG) and differential scanning calorimetric studies (DSC) (a) MWCNT, (b) $Co_{0.5}Mn_{0.5}Fe_2O_4$, MWCNT 1% (c) $Co_{0.5}Mn_{0.5}Fe_2O_4$, MWCNT 5% (d) $Co_{0.5}Mn_{0.5}Fe_2O_4$, MWCNT 9%

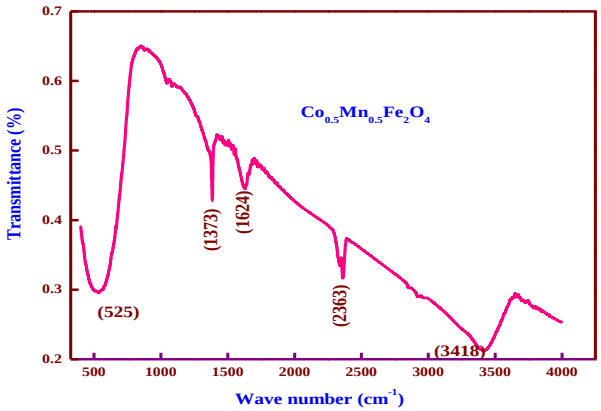

Fig. 4 FT-IR spectrum of $Co_{0.5}Mn_{0.5}Fe_2O_4$

FTIR spectroscopy is a very useful technique to deduce the structural investigation and redistribution of cations between octahedral and tetrahedral sites of the spinel structure in $Co_{0.5}Mn_{0.5}Fe_2O_4$ nanoparticles. The band around 1373 cm^{-1} is for C-H out of plane deformation

vibration. The adsorbed water is featured by bands at 3418 cm^{-1}. The bands at 2363 cm^{-1}, 1624 cm^{-1} are assigned to the O-H stretching and H-O-H bonding modes of vibration, respectively. The presence of band 525 cm^{-1} is attributed to the stretching vibration of tetrahedral and octahedral groups [47-49]. The sketch of the Fourier transform infrared spectroscopy is shown in Fig. 4.

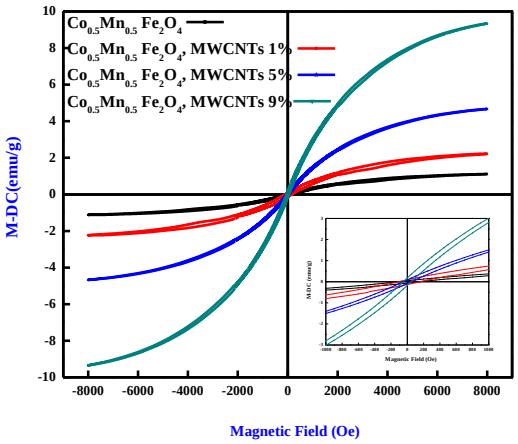

Fig.5 M-H curves for $Co_{0.5}Mn_{0.5}Fe_2O_4$ and multiwall carbon nanotubes composites.

The specific M-H curve for ferrite multiwall carbon nanotube composite obtained from physical property measurements (PPMs) technique is shown in Fig. 5. The sample exhibit linear magnetization with small coercivety indicating that ferrite nanoparticles are super paramagnetic the magnetic domains are based on randomly oriented non-interacting particles. The samples cannot fully saturate at 8KOe, this thing indicate the presence of super paramagnetic and single domain particles [47, 48].The values of saturation magnetization increased from 2.26 emu/g to 9.35emu/g with the increased percentage quantity of multiwall carbon nanotubes it may be due to the decoupling effect. The coercivety value for the Nano composite increases from 48 Oe to 152 Oe, showing increased in magnetization results from very well interaction between Nano crystalline $Co_{0.5}Mn_{0.5}Fe_2O_4$ and multiwall carbon nanotube.

4. Conclusions

Samples of Nano crystalline $Co_{0.5}Mn_{0.5}Fe_2O_4$ has been successfully synthesized using co-precipitation method and the effect of multiwall carbon nanotube composite have been studied. Lattice parameter, density and crystallite size decreases with the increase of MWCNTs concentration. Porosity increases with the increase of MWCNTs concentrations. DSC curves show the exothermic peaks at 636°C, 626 °C, 627 °C, and 628 °C due to the removal of hydrocarbon residues. XRD pattern indicates the ferrite is single phase with Face centered cubic structure. The saturation magnetization increases from 2.26emu/g to 9.35emu/g with the increase of multiwall carbon nanotubes due to the decoupling effect. The coercivity value increases from 48Oe to 152Oe. The thermal stability and loss in weight of the material increase with the addition amount of MWCNTs. The crystallite size range was 20nm to 35nm. Materials exhibit the super paramagnetic behavior as reported by Subhash B. Kondawar et al and G. Murtaza et al [50, 51]. Ferrite and MWCNTs composites are suitable for the application of electromagnetic devices, biomedical fields such as clinical diagnosis and electrochemical bio sensing. The presence of band 525cm^{-1} is attributed to the stretching vibration of tetrahedral and octahedral groups

Acknowledgement

Corresponding author (Ghulam Murtaza) is thankful to Higher Education Commission (HEC) of Pakistan for providing financial assistance through IRSIP scholarship and the Zhejiang University of China for providing opportunity to do work in Carbon Black Polymer Composite Lab (CBPCL).

References

[1] S. Iijima., Nature **354**, 56 (1991).
[2] W. A. De Heer, MRS Bulletin, **29**(4), 281 (2004).
[3] J. –P. Salvetat, G. Andrew, D. Briggs, J.-M. Bonard, R. R. Bacsa, A. J. Kulik, T. Stöckli, N. A. Burnham,L.Forró, Phys. Rev. Lett. **82**(5), 944 (1999).
[4] S. Berber, Y. –K. Kwon, D. Tomànek, Phys. Rev. Lett. **84**(20), 4613 (2000).
[5] T. W. Ebbesen, H. J. Lezec, H. Hiura, J. W. Bennett.H. F. Ghaemi, T. Thio, Nature, **382**(6586), 54 (1996).
[6] K. C. Han, H. D. Choi, T. J. Moon, W. S. Kim, J. Mater. Sci.**30**, 3567 (1995).
[7] M. R. Meshram, N. K. Agrawal, B. Sinha, P. S. Misra, Bull. Mater. Sci. **25**, 169 (2002).
[8] J. L. Dornan, D. Fiorani ,Magnetic Properties of Fine Particles (North-Holland, London, 1992).
[9] V. Blaskov, V. Petkov, V. Rusanov, L. M. Martinez, B. Martinez, J. S. Munoz and M. Mikhov, J. Magn. Magn. Mater.**162**, 331 (1996),.
[10] K. S. Baek, H. N. Ok, J. C. Sur, Phys. Rev. B **39**, 2800 (1989).
[11] S. N. Okuno, S. Hashimoto, K. Inomata, J. Appl. Phys. **71**, 5926 (1992).
[12] T. Pannaparayil., R. Marande, , S. Komarneni., J. Appl. Phys. **69**, 5349 (1991).
[13] M. Rozman., M. Drofenik., J. Am. Ceram. Soc **78**, 2449 (1995).
[14] S. Komarneni., E. Fregeau, E. Breval., R. Roy, J. Am. Ceram. Soc. **71**, c-26- (1998).
[15] M. Sisk., I. Kilbride, A. J. barker, J. Mater. Sci. Lett **14**, 153 (1995).
[16] M. Kiyama. Bull. Chem. Soc. Jpn. **51**, 134 (1978).
[17] T. Katsura, Y. Tamura., G.S. Chyo, Bull.Chem. Soc, Jpn.**52**, 96 (1979).
[18] K. Kaneko., T. Kastura., Bull. Chem. Soc. Jpn. **52**, 1080 (1979).
[19] K. Kaneko, K. Takei., Y. Tamura, T. Kanzaki, T. Kastura, Bull. Chem. Soc. Jpn. **52,** 1080 (1979).
[20] Y. Tamura, U. Rasyid, T. Kastura, J. Chem. Soc., Dalton Trans, **53**, 2125 (1980).
[21] J. G. Lee, J. Y. Park, C. S. Kim. J. Mater. Sci. **33**, 3965 (1998).
[22] S. G. Christoskova, M. Stoyanova, M. Georgieva, Appl. Catal. A **208**, 235 (2001).
[23] C. O. Arean, M. P. Mentruit, E. E. Platero, F.X.L.I . Xamena., J. B. Parra, Mater. Lett. **39,** 22 (1999).
[24] C.S. Kim, Y.S. Yi., K.T. Park., H. Namgung, J. G. Lee, J. Appl. Phys. **85**, 5223 (1999) .
[25] H. F. Yu, A. M. Gadalla., J. Mater. Res. **11**, 663 (1996).
[26] N. Moumen, O. Veillet., M. P. Pileni., J. Magn. Magn. Mater. **149,** 67 (1995).
[27] N. S. Kommareddi., M. Tata., V. T John., G. L. McPherson., M. F Herman, Y.S. Lee, O.J., J. A. Akkara., D. L. Kaplan, Chem.Mater.**8**, 801 (1996) -809.
[28] M. A. Lopez. –Quintela.., J. Rivas., J. Colloid Interface Sci. **158**, 446 (1993).
[29] J. Ding., P. G. McCormick., P. G. R. Street, Solid State Commun. **95**, 31 (1995).
[30] J. Ding, T. Reynolds, W.F. Miao, Appl. Phys. Lett. **65**, 3135 (1994).
[31] J. Ding, P.G. McCormick, R. Street, J. Magn. Magn. Mater.**171**, 309 (1997).
[32] Y Shi, J. Ding., X. Liu., J. Wang, J. Magn. Magn.Mater. **205**, 249 (1999).
[33] N. Ikenaga, Y. Ohgaito, H. Matsushima, T. Suzuki, Fuel **83**, 661 (2004).
[34] C. W. Jung, P. Jacobs, Magnetic Resonance Imaging **13**, 661 (1995) -674.
[35] J. P. Liu, Springer Verlag, 2009.
[36] N. A. Brusentsov, V. Gogosov, T. Brusentsova, A. Sergeev, N. Jurchenko, A. A. Kuznetsov, O. A. Kuznetsov, L. Shumakov, J. Magn. Magn. Mater. **225**, 113 (2001).
[37] N. Guigue-Millot, S. Begin-Colin, Y. Champion, M. H'tch, G. Le Caer, P. Perriat, J. solid

stat. chem. **170**, 30 (2003).
[38] M. Mouallem-Bahout, S. Bertrand, O. Pena, J. solid stat. chem, **178**, 1080 (2005)
[39] W. Zhou, Y. H. Ooi, R. Russo., P. Papanek., D. E. Luzzi, J. E. Fischer., M. J. Bronikowski. P. A. Willis., R. E. Smalley., Chem. Phys. Lett. **350**, 6 (2001).
[40] K. Tohji, T. Goto., H. Takahashi., Y. Shinoda., N. Shimizu., B. Jeyadevan., I. Matsuoka, Y. Saito., A. Kasuya, T. Ohsuna, K. Hiraga, Y. Nishina, Nature, **383,** 679 (1996).
[41] E. Dujardin., T. W. Ebbessen., A. Krishnan, M. M. Treacy, J. Adv. Mater.**10**, 611 (1998).
[42] M. H. Yousefi, S. Manouchehri, A. Arab, M. Mmozaffari, Gh. R. Amiri, J. Amighian, Material Research Bulletin **45**, 1792 (2010).
[43] J. Smit, H. P. J. Wijin, Ferrites, John Wiley, New York (1959) 233.
[44] S. T. Alone, Sagar E. Shirsath, R. H. Kadam, K. M. Jadhav, J. Alloys and Compounds **509**, 5055 (2011).
[45] C.Wang, Y. Shen, X. Wang, H. Zhang, A. Xie, Materials Sc. in Sem. Processing, **16**, 77 (2013).
[46] Y. Zhang, D. Wen, Materials Sc. Engg B, **172**, 331 (2010).
[47] J. D. L. C. P. Bean, J. Appl. Phys. **30**, 1205 (1959).
[48] R. R. Shahraki, M. Ebrahimi, S. A. S. Ebrahimi, S. M. Masoudpanah, J,Magn. Magnet.Mater.**324**, 3762 (2012).
[49] H. Soleimani, Z. Abbas, N. Yahya, K. Shameli, H. Soleimani, P. Shabanzadeh, Int. J. Mol. Sci. **13**, 8540 (2012).
[50] S. B. Kondawar, A. I. Nandapure, B. I. Nandapure, Adv. Mat. Lett. **5**(6), 339 (2014).
[51] G. Murtaza, I. Ahmad, A. Hakeem, P. Mao, X. Guohua, M. T. Farid, G. Mustafa, M. Kanwal, M. Hussain, Digest Journal of Nanomaterials and Biostructures, **10**(4),1393 (2015).